THE JOURNAL OF PHYSICAL CHEMISTRY A
A JOURNAL OF THE AMERICAN CHEMICAL SOCIETY

pubs.acs.org/JPCA Article

Fundamental Vibrational Frequencies and Spectroscopic Constants of Substituted Cyclopropenylidene (c-C_3HX, X = F, Cl, CN)

Brent R. Westbrook, Dev J. Patel, Jax D. Dallas, G. Clark Swartzfager, Timothy J. Lee, and Ryan C. Fortenberry*

Cite This: J. Phys. Chem. A 2021, 125, 8860–8868 Read Online

ACCESS | Metrics & More | Article Recommendations | Supporting Information

ABSTRACT: The recent detection of ethynyl-functionalized cyclopropenylidene (c-C_3HC_2H) has initiated the search for other functional forms of cyclopropenylidene (c-C_3H_2) in space. There is existing gas-phase rotational spectroscopic data for cyano-cyclopropenylidene (c-C_3HCN), but the present work provides the first anharmonic vibrational spectral data for that molecule, as well as the first full set of both rotational and vibrational spectroscopic data for fluoro- and chloro-cyclopropenylidenes (c-C_3HF and c-C_3HCl). All three molecules have fundamental vibrational frequencies with substantial infrared intensities. Namely, c-C_3HCN has a moderately intense fundamental frequency at 1244.4 cm^{-1}, while c-C_3HF has two large intensity modes at 1765.4 and 1125.3 cm^{-1} and c-C_3HCl again has two large intensity modes at 1692.0 and 1062.5 cm^{-1}. All of these frequencies are well within the spectral range covered by the high-resolution EXES instrument on NASA's Stratospheric Observatory for Infrared Astronomy (SOFIA). Further, all three molecules have dipole moments of around 3.0 D in line with c-C_3H_2, enabling them to be observed by pure rotational spectroscopy, as well. Thus, the rovibrational spectral data presented herein should assist with future laboratory studies of functionalized cyclopropenylidenes and may lead to their interstellar or circumstellar detection.

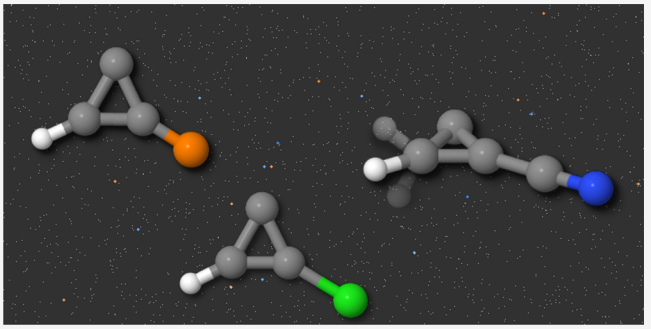

INTRODUCTION

Cyclopropenylidene (c-C_3H_2) is highly abundant in the interstellar medium (ISM)[1−3] and has recently been detected in the atmosphere of Saturn's moon Titan.[4] Since its interstellar discovery in 1985 through radioastronomical observation, c-C_3H_2 has paved the way for the observation of other, related molecules, including its singly and doubly deuterated forms and ^{13}C isotopologues.[5−7] Most hydrocarbons are nonpolar or weakly polar, making them poor targets for rotational spectroscopy. However, c-C_3H_2's lack of a third hydrogen lowers its symmetry, gives it a large dipole moment of 3.32 D,[8] and makes it rotationally observable. This feature allows c-C_3H_2 to serve as a potential indicator for other rotationally dark monocyclic or polycyclic aromatic hydrocarbons (PAHs) in the ISM. In addition to serving as an indicator, c-C_3H_2 may also be a building block of these larger PAHs.[3]

One proposed mechanism for PAH formation in the ISM is the ethynyl (C_2H) addition mechanism,[9] wherein a sequence of ethynyl additions to small hydrocarbons can yield increasingly complex PAH molecules. The recent detection of ethynyl-functionalized c-C_3H_2 (c-C_3HCCH) in the Taurus Molecular Cloud[10] lends potential support to such a proposal. The same mechanism may also help to explain the unexpectedly large abundances of cyclopentadiene and indene also detected in the same study,[10] but further work is needed to provide more conclusive evidence for such a process.

In the meantime, the search is now afoot for other functionalized forms of c-C_3H_2. The interstellar detection of benzonitrile in 2018[11] and the abundance of the cyanide radical (CN), again in both Titan's atmosphere and the ISM,[12,13] make CN a particularly appealing functional group. The interstellar abundance of the protonated[14] and anionic[15] forms of CN, namely HCN and CN^-, offer additional formation pathways for cyanated c-C_3H_2, further bolstering the appeal. The fact that the addition of CN should induce a substantial dipole moment in even totally nonpolar molecules means it should increase their observability by rotational spectroscopy as well. Further, the rotational spectrum of c-C_3HCN has been previously observed experimentally,[16] offering comparable data for benchmarking computational results. The linear, triplet HC_4N isomer has also been observed in the laboratory,[17] but MP2/D95** computations put this

Received: July 23, 2021
Revised: September 14, 2021
Published: October 5, 2021

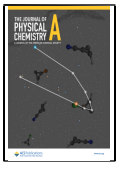

https://doi.org/10.1021/acs.jpca.1c06576
J. Phys. Chem. A 2021, 125, 8860−8868

isomer 11 kcal/mol higher in energy.[18] Similar linear cyanopolyyne chains (HC_nN) are well-known in the laboratory and in space,[17,19,20] but the cyclic variants have heretofore evaded astronomical detection. Thus, the present work provides the first fundamental vibrational spectroscopic data to aid in the detection of c-C_3HCN in space.

CN's high electronegativity and propensity for external single-bond formation means it functions much like the halogens. Consequently, another appealing direction of c-C_3H_2 functionalization is to replace one of the hydrogen atoms on c-C_3H_2 with fluorine or chlorine. Molecules containing chlorine[21−25] are relatively common in space, and the sizable abundance of chlorine in general[26] makes c-C_3HCl a good target of detection. Fluorine is substantially less abundant, but fluorinated molecules are known in the ISM,[27−29] and fluorine's ability to induce a larger dipole moment means that these molecules should be detectable even in lower concentrations. Regardless, both fluorine and chlorine should yield substantial dipole moments in the functionalized c-C_3H_2 molecule, making them readily observable by both vibrational and rotational spectroscopies if their spectral properties can be determined.

The best balance of accuracy and computational cost in theoretical rovibrational analysis is the quartic force field (QFF). QFFs are fourth-order Taylor series expansions of the internuclear potential energy portion of the Watson Hamiltonian.[30] When conjoined to coupled cluster theory at the singles, doubles, and perturbative triples level[31] within the F12b explicitly correlated formalism [CCSD(T)-F12b][32,33] and a triple-ζ basis set, QFFs can achieve agreement to within 5−7 cm^{-1} of gas-phase experimental vibrational frequencies.[34−38] The accuracy of the rotational data is typically less impressive, especially compared to more expensive composite methods,[39] but the availability of experimental rotational data for c-C_3HCN can serve to benchmark the performance of the QFFs for the other two molecules given the similar structures. Regardless, the fundamental vibrational frequencies provided here will be invaluable in elucidating the spectra gathered by the existing Stratospheric Observatory for Infrared Astronomy (SOFIA) and the upcoming James Webb Space Telescope (JWST).

METHODS

Optimized geometries, dipole moments, and vibrational frequencies are computed using the Molpro 2020.1 software package[40] at the CCSD(T)-F12b/cc-pVTZ-F12 level of theory,[34,41,42] hereafter referred to as F12-TZ. The MP2/aug-cc-pVDZ level of theory[43,44] is used to compute the double-harmonic and anharmonic infrared intensities within the Gaussian16[45] suite of programs. This level of theory has previously been shown to be reliable for semiquantitative descriptions of the fundamental intensities.[46,47]

Following the F12-TZ geometry optimization, displacements of 0.005 Å or rad are taken from the optimized geometry to map out the QFF. The symmetry internal coordinates along which these displacements are taken for the c-C_3HCN molecule are shown below, using the numbering scheme from the molecular geometry depicted in Figure 1. Of note here is the fact that the C_5-N_6 stretch is not treated explicitly to avoid introducing a linear dependency in the coordinate system. Instead, the C_4-N_6 bond is used in its place.

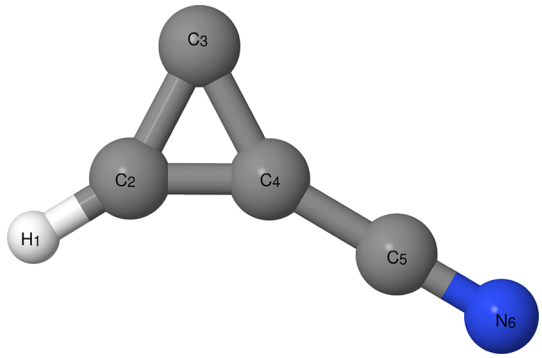

Figure 1. c-C_3HCN reference geometry.

$$S_1(a') = r(H_1-C_2) \quad (1)$$

$$S_2(a') = r(C_2-C_3) \quad (2)$$

$$S_3(a') = r(C_3-C_4) \quad (3)$$

$$S_4(a') = r(C_4-C_5) \quad (4)$$

$$S_5(a') = r(C_4-N_6) \quad (5)$$

$$S_6(a') = \angle(H_1-C_2-C_3) \quad (6)$$

$$S_7(a') = \angle(C_2-C_3-C_4) \quad (7)$$

$$S_8(a') = \angle(C_3-C_4-C_5) \quad (8)$$

$$S_9(a') = \angle(C_3-C_4-N_6) \quad (9)$$

$$S_{10}(a'') = \tau(H_1-C_2-C_3-C_4) \quad (10)$$

$$S_{11}(a'') = \tau(C_2-C_3-C_4-C_5) \quad (11)$$

$$S_{12}(a'') = \tau(C_2-C_3-C_4-N_6) \quad (12)$$

Similarly, the internal coordinate scheme for the c-C_3HX molecules is shown below, this time with numbering consistent with Figure 2:

$$S_1(a') = r(H_1-C_2) \quad (13)$$

$$S_2(a') = r(C_2-C_3) \quad (14)$$

$$S_3(a') = r(C_3-C_4) \quad (15)$$

$$S_4(a') = r(C_4-X_5) \quad (16)$$

$$S_5(a') = \angle(H_1-C_2-C_3) \quad (17)$$

$$S_6(a') = \angle(C_2-C_3-C_4) \quad (18)$$

$$S_7(a') = \angle(C_3-C_4-X_5) \quad (19)$$

$$S_8(a'') = \tau(H_1-C_2-C_3-C_4) \quad (20)$$

$$S_9(a'') = \tau(C_2-C_3-C_4-X_5) \quad (21)$$

In all cases, F12-TZ single-point energies are computed at each of these displaced geometries, again utilizing the Molpro 2020.1 software package. Following this, a least-squares fitting procedure with a sum of squared residuals less than 8×10^{-15} au^2 in all cases is used to yield the equilibrium geometry and the force constants that are refit to this new geometry. Then, the symmetry internal coordinate force constants are converted

https://doi.org/10.1021/acs.jpca.1c06576
J. Phys. Chem. A 2021, 125, 8860−8868

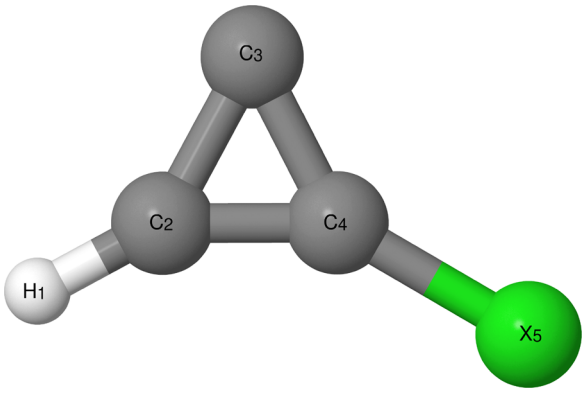

Figure 2. c-C_3HX reference geometry for X = F, Cl.

back into Cartesian coordinates using the INTDER program.[48] The SPECTRO program[49] uses the Cartesian force constants to produce the fundamental frequencies and rotational constants via rotational, rovibrational, and vibrational perturbation theory at second order (VPT2).[50,51] Type 1 and 2 Fermi resonances and Fermi resonance polyads, Coriolis resonances, and Darling−Dennison resonances are accounted for to further boost the accuracy of the rovibrational data.[52] The Fermi resonances and polyads are reported in Tables S1−S6.

Larger step sizes of 0.010 and 0.020 Å or rad are also used in the out-of-plane symmetry internal coordinates in order to alleviate potential problems brought about by known issues with out-of-plane bending (OPB) motions in hydrocarbons, and in c-C_3H_2 in particular.[53−55] Step sizes of 0.010 and 0.020 have been previously shown to mitigate this problem for the related c-$(CH)C_3H_2^+$ molecule and for c-C_3H_2 itself.[56,57] The out-of-plane coordinates correspond to the torsional coordinates S_{10}, S_{11}, and S_{12} in c-C_3HCN and to S_8 and S_9 in c-C_3HF and c-C_3HCl, respectively.

RESULTS AND DISCUSSION

Geometrical Parameters and Rotational Constants. The agreement of the computed principal rotational constants for c-C_3HCN with the available gas-phase experimental values is quite good. The F12-TZ QFF *B* and *C* rotational constants of 3497.1 and 3168.3 MHz, as shown in Table 1, are within 16.3 MHz (0.46%) and 15.3 MHz (0.48%), respectively, of the experimental values at 3513.4 and 3183.6 MHz. This is well within the expected accuracy of even much more expensive QFF methodologies, which can only reliably yield *B* and *C* constants within about 20 MHz[39] of gas-phase experiment. While the *A* constant is farther off at a difference of just under 200 MHz between the predicted 34081.4 MHz and the experimental 34281.3 MHz, this is still only a relative difference of 0.58%. Because of their larger magnitudes, computed *A* rotational constants are known to experience larger absolute errors than the *B* and *C* constants.[39] This trend is similar to that observed in a previous study on c-C_3H_2 itself, in which the rotational constants were found to agree very well with experiment, suggesting that F12-TZ QFFs may effectively handle the rotational spectra of c-C_3H_2 and its related molecules.[54]

Further evidence for the good performance of the present QFFs is the agreement in the available quartic distortion coefficients presented in Table 2. The F12-TZ QFF values of 323.554 Hz for Δ_J and 29.857 kHz for Δ_{JK} are within 6 Hz and 1 kHz of the gas-phase values, respectively. While experimental values are unavailable to benchmark the c-C_3HF and c-C_3HCl molecules directly, their structures and internal coordinate definitions are similar to those of both c-C_3HCN and the previously studied c-C_3H_2, suggesting that the QFF methodology should yield reliable rotational constants for them, too. Similarly, the exceptional performance of the F12-TZ QFF in the rotational constants supports the corresponding vibrational frequencies, which are already expected to be reliable at this level of theory.[34−38]

The principal rotational constants for c-C_3HF and c-C_3HCl are shown in Table 1, and their quartic and sextic distortion coefficients are shown in Table 2. The equilibrium and vibrationally averaged geometrical parameters, as well as the dipole moment, of c-C_3HCN are shown in Table 3. Those of c-C_3HF and c-C_3HCl are given in Table 4. The Cartesian coordinates for all three molecules and the corresponding dipole moment components are presented in Tables S7−S9.

Vibrational Frequencies. With respect to vibrational spectroscopy, all three molecules have frequencies with sizable infrared intensities, as shown in Tables 5 and 6. c-C_3HF and c-C_3HCl, in particular, have C_3-C_4 stretching (ν_2) and $C_2-C_3-C_4$ bending (ν_4) motions with intensities (*f*) near 100 km mol^{-1}. The $C_2-C_3-C_4$ bend of c-C_3HCN is also its most intense motion, but the MP2/aug-cc-pVDZ computations put its intensity much lower at only 31 km mol^{-1}. Nevertheless, even this intensity should make c-C_3HCN detectable by infrared spectroscopy, as well. With the goal of astronomical detection in mind, the most intense modes of c-C_3HF occur at 1765.2 and 1125.3 cm^{-1} for ν_2 and ν_4, respectively, while the same modes for c-C_3HCl have values of 1692.0 and 1062.6 cm^{-1}. For c-C_3HF, these frequencies have intensities greater than 130 km mol^{-1}, while those for c-C_3HCl are slightly lower but still greater than 80 km mol^{-1}. A common point of comparison for these intensities is the antisymmetric stretch of water, which has an infrared intensity around 70 km mol^{-1}, and both of these molecules have fundamental frequencies with intensities above that threshold.

c-C_3HCN, on the other hand, only has a single intensity greater than 30 km mol^{-1}. The ν_4 $C_2-C_3-C_4$ bend at 1244.4 cm^{-1} has an intensity of 31 km mol^{-1}, which is about half of the intensity for the aforementioned antisymmetric stretch in water. This should still be sufficient for astronomical detection in the infrared, but the signal available for c-C_3HCN will not be as vivid as for its halogenated counterparts in this region of the electromagnetic spectrum. The only other modes with substantial intensities for c-C_3HCN are its hydrogen and nitrogen OPB modes and the nitrogen in-plane bend (IPB). All three of these modes have comparable intensities around 10 km mol^{-1} and frequencies of 890.7, 219.3, and 201.6 cm^{-1} for the H OPB, N OPB, and N IPB, respectively.

Although Tables 5 and 6 list both the harmonic and anharmonic MP2/aug-cc-pVDZ infrared intensities, as found previously,[46,47] there is shown here to be little benefit in computing the anharmonic intensities at this level of theory. Both give the same qualitative intensity values, and this level of theory can only be semiquantitative at best. The largest disagreement in the present data set occurs between ω_2 and ν_2 for c-C_3HF, where the harmonic intensity of 198 km mol^{-1} is 75 km mol^{-1} greater than the anharmonic value of 123 km mol^{-1}. Regardless of this large disparity, the mode is still indicated as one of the most intense, which is the best this level of theory can really offer. The intensity computations have also

https://doi.org/10.1021/acs.jpca.1c06576
J. Phys. Chem. A 2021, 125, 8860−8868

Table 1. Principal Rotational Constants (in MHz)

	c-C_3HCN			c-C_3HF			c-C_3HCl		
	0.005	0.010	expt[a]	0.005	0.010	0.020	0.005	0.010	0.020
A_e	34278.9	34278.9		33568.4	33568.4	33568.4	34061.2	34061.5	34061.2
B_e	3500.7	3500.7		7627.3	7627.3	7627.3	4135.3	4134.4	4135.3
C_e	3176.3	3176.3		6215.0	6215.0	6215.0	3687.4	3687.1	3687.4
A_0	34081.6	34081.4	34281.3348(14)	33313.4	33313.3	33313.3	33825.4	33825.6	33825.2
B_0	3497.0	3497.1	3513.3728(3)	7598.1	7598.2	7598.3	4122.4	4121.8	4122.5
C_0	3168.3	3168.3	3183.5898(3)	6177.6	6177.7	6177.7	3670.7	3670.2	3670.7
A_1	33956.9	33956.7		33224.6	33224.6	33224.5	33720.3	33720.5	33720.1
B_1	3494.6	3494.7		7588.7	7588.8	7588.9	4119.1	4118.5	4119.2
C_1	3165.3	3165.4		6168.3	6168.5	6168.5	3666.9	3666.4	3666.9
A_2	34089.7	34089.5		33256.2	33256.2	33256.1	33776.7	33776.9	33776.4
B_2	3481.8	3481.9		7551.3	7551.5	7551.5	4104.6	4104.0	4104.7
C_2	3155.9	3155.9		6146.4	6146.5	6146.6	3656.4	3655.9	3656.4
A_3	34032.6	34032.3		33393.5	33393.5	33393.4	33808.9	33808.9	33808.7
B_3	3484.8	3484.9		7569.6	7569.8	7569.8	4114.6	4114.0	4114.6
C_3	3158.1	3158.1		6164.0	6164.1	6164.1	3667.0	3666.5	3667.0
A_4	33995.9	33996.1		32997.2	32997.1	32997.1	33757.1	33757.4	33756.9
B_4	3494.6	3494.7		7605.8	7605.9	7606.0	4119.5	4118.9	4119.6
C_4	3164.2	3164.3		6157.2	6157.3	6157.3	3659.6	3659.2	3659.7
A_5	34082.4	34081.5		33293.3	33293.3	33293.2	34675.6	34676.2	34675.4
B_5	3492.9	3493.0		7685.9	7686.1	7686.1	4126.2	4125.6	4126.3
C_5	3162.1	3162.2		6173.9	6174.0	6174.0	3669.5	3669.0	3669.5
A_6	34655.3	34655.9		33307.5	33307.3	33307.2	32754.4	32753.9	32753.7
B_6	3499.4	3499.5		7510.4	7510.8	7510.9	4122.2	4121.7	4122.4
C_6	3167.9	3167.9		6180.9	6181.1	6181.2	3672.2	3671.8	3672.4
A_7	33379.6	33378.9		33198.7	33198.7	33198.6	33799.3	33799.5	33799.1
B_7	3495.9	3496.1		7595.8	7595.9	7596.0	4111.5	4110.9	4111.5
C_7	3169.3	3169.4		6169.6	6169.7	6169.8	3661.9	3661.4	3661.9
A_8	34054.3	34054.2		33457.0	33457.0	33457.0	33674.9	33675.0	33674.6
B_8	3493.0	3493.0		7620.4	7620.6	7620.7	4128.5	4127.9	4128.6
C_8	3163.8	3163.8		6170.3	6170.4	6170.4	3678.9	3678.5	3679.0
A_9	33976.8	33976.5		33182.2	33182.1	33182.1	33990.4	33990.6	33990.2
B_9	3501.8	3501.9		7596.3	7596.6	7596.6	4129.5	4128.9	4129.6
C_9	3174.2	3174.3		6192.4	6192.6	6192.7	3669.9	3669.4	3670.0
A_{10}	34211.6	34211.4							
B_{10}	3501.2	3501.2							
C_{10}	3169.9	3170.0							
A_{11}	33912.2	33911.9							
B_{11}	3506.3	3506.4							
C_{11}	3179.3	3179.4							
A_{12}	34237.5	34237.3							
B_{12}	3510.2	3510.3							
C_{12}	3173.6	3173.7							

[a]From ref 58.

been repeated at the B3LYP/aug-cc-pVTZ level[44,59−61] to verify the accuracy of the MP2 data. These results are presented in Table S10. The largest deviations between the MP2 and B3LYP results occur in ω_4 and ν_4 of c-C_3HCl, with differences of 22 and 19 km mol^{-1}, respectively, but the vast majority of the values differ by no more than 1 km mol^{-1}, again suggesting that the MP2 results are sufficiently accurate to be qualitatively useful for a very low computational cost.

A final, useful comparison given the recent detection of benzonitrile in the ISM[11] is the C≡N stretching frequency between benzonitrile and c-C_3HCN. Gas-phase experimental data for benzonitrile puts its C≡N stretching frequency at 2242 cm^{-1}, with a "very strong" intensity.[62] This value is nearly identical to the C≡N stretch reported here for c-C_3HCN at 2241.0 cm^{-1}, which would make it difficult to separate the two signals if both molecules were found in one place. However, the near-zero intensity of c-C_3HCN's C≡N stretch makes it a poor indicator for the molecule anyway. A more useful mode to look for in c-C_3HCN is its C═C stretch at 1244.4 cm^{-1}, which has the largest computed intensity for this molecule at 31 km mol^{-1}.

The small intensity of c-C_3HCN's C≡N stretch is somewhat surprising given the strong intensity of the corresponding mode in benzonitrile. In the case of c-C_3HCN, the C≡N stretch causes virtually no change in the net dipole moment. Computing the dipole moment in a scan of C_5 displacements along the C_5−N_6 bond length from −0.5 to 0.5 Å in 0.1 Å increments yields a maximum dipole moment of 3.74 D when the carbon is 0.4 Å farther from the nitrogen, which is only 0.28 D (8%) greater than the value for the

https://doi.org/10.1021/acs.jpca.1c06576
J. Phys. Chem. A 2021, 125, 8860−8868

Table 2. Quartic and Sextic Distortion Coefficients

	c-C_3HCN				c-C_3HF				c-C_3HCl			
	units	0.005	0.010	expt[a]	units	0.005	0.010	0.020	units	0.005	0.010	0.020
Δ_J	Hz	323.516	323.554	317(6)	kHz	2.042	2.042	2.042	Hz	713.178	712.870	713.178
Δ_{JK}	kHz	29.866	29.857	30.16(14)	kHz	34.057	34.057	34.057	kHz	20.093	20.085	20.093
Δ_K	kHz	106.057	106.039		kHz	107.406	107.406	107.406	kHz	120.094	120.121	120.094
δ_J	Hz	33.756	33.762		Hz	415.938	415.938	415.938	Hz	83.801	83.753	83.801
δ_K	kHz	16.427	16.423		kHz	22.910	22.910	22.910	kHz	12.514	12.509	12.514
Φ_J	μHz	8.171	8.232		μHz	464.779	464.779	464.776	μHz	−26.597	−26.586	−26.598
Φ_{JK}	mHz	162.957	162.855		mHz	134.021	134.021	134.020	mHz	55.076	55.036	55.076
Φ_K	Hz	3.388	3.386		mHz	206.386	206.383	206.388	mHz	525.679	526.233	525.674
Φ_{KJ}	Hz	−3.372	−3.370		mHz	−106.564	−106.555	−106.554	mHz	−327.682	−327.707	−327.683
ϕ_j	μHz	7.081	7.104		μHz	278.506	278.506	278.505	μHz	17.086	17.075	17.086
ϕ_{jk}	mHz	82.008	81.960		mHz	70.785	70.784	70.784	mHz	28.261	28.241	28.261
ϕ_k	Hz	6.173	6.170		Hz	2.274	2.274	2.274	Hz	2.167	2.166	2.167

[a]From ref 58.

Table 3. Geometrical Parameters (in Å or Degrees) and Dipole Moment (in D) of c-C_3HCN

	0.005	0.010
$r_e(H_1-C_2)$	1.0770770	1.0770770
$r_e(C_4-N_6)$	2.5701599	2.5701599
$r_e(C_4-C_5)$	1.4092787	1.4092787
$r_e(C_3-C_4)$	1.4297231	1.4297231
$r_e(C_2-C_3)$	1.4208127	1.4208127
$\angle_e(C_4-C_3-N_6)$	148.2660543	148.2660441
$\angle_e(C_4-C_3-C_5)$	148.2806680	148.2806598
$\angle_e(C_3-C_2-C_4)$	55.5147476	55.5147474
$\angle_e(C_2-H_1-C_3)$	148.9913399	148.9913406
$r_0(H_1-C_2)$	1.0771442	1.0771338
$r_0(C_4-N_6)$	2.5706912	2.5706680
$r_0(C_4-C_5)$	1.4118935	1.4119118
$r_0(C_3-C_4)$	1.4334708	1.4334697
$r_0(C_2-C_3)$	1.4270076	1.4270136
$\angle_0(C_4-C_3-N_6)$	148.2196379	148.2238898
$\angle_0(C_4-C_3-C_5)$	148.2506687	148.2538324
$\angle_0(C_3-C_2-C_4)$	55.4570545	55.4557651
$\angle_0(C_2-H_1-C_3)$	149.0821546	149.0797165
μ	3.46	

optimized structure at 3.46 D. In benzonitrile, any change in the C−N bond length moves directly along the net dipole moment, giving the stretching motion a large intensity. In contrast, the lone pair on the apical c-C_3HCN carbon, C_3, roughly balances the top-to-bottom component of the dipole moment, leaving the net dipole to point from the center of the molecule toward the side with the CN group but not directly along the C−N bond. Hence, the C≡N stretch does not induce a large enough change in the dipole moment to give it a substantial intensity. In short, the large dipole moment of 3.32 D in unsubstituted c-C_3H_2 mostly nullifies the contribution of the CN, while benzene's lack of a net dipole moment means the CN has a much larger impact on the dipole and, in turn, on the intensity of the C≡N stretching mode, in benzonitrile.

OPB Issue. Previous work on c-$(CH)C_3H_2^+$[56] and c-C_3H_2[57] has shown that the well-known OPB issue in multiply bonded hydrocarbons[55] can be mitigated by using larger step sizes to map the QFF. As such, the QFFs in the present work are repeated using step sizes of 0.010 and 0.020 rad in the OPB coordinates in order to check the impact of the step size on the spectroscopic constants of these related molecules. As shown in Tables 1 and 2, the effect of the varied step sizes is unsurprisingly negligible for the principal rotational constants as well as the quartic and sextic distortion coefficients. Similarly, there is virtually no effect on the harmonic vibrational frequencies of Table 5, with the largest deviations consisting of 0.1 cm^{-1} each. This is in line with previous work that pointed to numerical instability as the root of the OPB problem for similar molecules.[57] The numerical issues are exacerbated as the order of the force constants involved increases. Consequently, the harmonic frequencies, which utilize only the second-order force constants, are nearly

Table 4. Geometrical Parameters (in Å or Degrees) and Dipole Moments (in D) of c-C_3HF and c-C_3HCl

	c-C_3HF			c-C_3HCl		
	0.005	0.010	0.020	0.005	0.010	0.020
$r_e(H_1-C_2)$	2.4072434	2.4072434	2.4072434	2.4049895	2.4049895	2.4049895
$r_e(C_4-X_5)$	1.3001930	1.3001930	1.3001930	1.6770515	1.6770722	1.6770515
$r_e(C_3-C_4)$	1.3158335	1.3158335	1.3158335	1.3229777	1.3232236	1.3229777
$r_e(C_2-C_3)$	1.4456655	1.4456655	1.4456655	1.4303617	1.4303617	1.4303617
$\angle_e(H_1-C_2-C_3)$	20.2385471	20.2385471	20.2385474	19.0305584	19.0305584	19.0305586
$r_0(H_1-C_2)$	2.4158049	2.4158415	2.4158523	2.4126174	2.4126586	2.4126699
$r_0(C_4-X_5)$	1.3044231	1.3044120	1.3044094	1.6810828	1.6810973	1.6810748
$r_0(C_3-C_4)$	1.3201097	1.3201087	1.3201086	1.3266581	1.3269029	1.3266565
$r_0(C_2-C_3)$	1.4540564	1.4540500	1.4540483	1.4377661	1.4377607	1.4377589
$\angle_0(H_1-C_2-C_3)$	20.2884764	20.2853599	20.2844207	19.0477931	19.0439928	19.0429044
μ		2.99			3.06	

https://doi.org/10.1021/acs.jpca.1c06576
J. Phys. Chem. A 2021, 125, 8860−8868

Table 5. F12-TZ QFF Vibrational Frequencies and MP2/aug-cc-pVDZ Infrared Intensities of c-C_3HF and c-C_3HCl (Frequencies in cm^{-1} and Intensities in km mol^{-1})

		c-C_3HF				c-C_3HCl			
mode	description	0.005	0.010	0.020	f	0.005	0.010	0.020	f
$\omega_1(a')$	C−H stretch	3271.2	3271.2	3271.2	9	3264.8	3264.8	3264.8	5
$\omega_2(a')$	C_3C_4 stretch	1820.6	1820.6	1820.6	198	1710.0	1710.0	1710.0	89
$\omega_3(a')$	C_2−C_3 stretch	1393.9	1393.9	1393.9	10	1310.8	1310.8	1310.8	29
$\omega_4(a')$	C_2−C_3−C_4 bend	1156.2	1156.2	1156.2	139	1092.9	1092.8	1092.9	97
$\omega_5(a')$	H−C−C bend	944.8	944.8	944.8	7	921.7	921.7	921.7	3
$\omega_6(a'')$	H OPB	909.3	909.3	909.3	17	893.8	893.8	893.8	10
$\omega_7(a')$	C−X stretch	790.4	790.4	790.4	22	591.2	591.2	591.2	17
$\omega_8(a'')$	X OPB	466.4	466.4	466.4	5	395.1	395.2	395.1	1
$\omega_9(a')$	X IPB	465.7	465.7	465.7	12	351.9	351.9	351.9	9
$\nu_1(a')$	C−H stretch	3138.9	3138.8	3138.8	7	3128.9	3128.8	3128.8	3
$\nu_2(a')$	C_3−C_4 stretch	1766.6	1765.4	1765.2	123	1692.0	1692.0	1692.0	64
$\nu_3(a')$	C_2−C_3 stretch	1362.3	1362.2	1362.2	9	1282.8	1282.6	1282.7	28
$\nu_4(a')$	C_2−C_3−C_4 bend	1125.3	1125.3	1125.3	139	1062.5	1062.5	1062.6	96
$\nu_5(a')$	H−C−C bend	923.1	922.7	922.6	7	898.7	898.2	898.1	3
$\nu_6(a'')$	H OPB	898.3	894.3	893.9	18	881.8	879.7	879.5	10
$\nu_7(a')$	C−X stretch	771.3	771.1	771.0	21	581.0	581.0	581.1	17
$\nu_8(a'')$	X OPB	459.6	459.5	459.5	4	392.6	392.4	392.5	1
$\nu_9(a')$	X IPB	462.9	461.2	460.9	11	347.7	347.7	347.8	9

Table 6. F12-TZ QFF Vibrational Frequencies and MP2/aug-cc-pVDZ Infrared Intensities of c-C_3HCN (Frequencies in cm^{-1} and Intensities in km mol^{-1})

mode	description	0.005	0.010	f
$\omega_1(a')$	C−H stretch	3271.6	3271.2	7
$\omega_2(a')$	C≡N stretch	2280.2	2280.1	1
$\omega_3(a')$	C_3−C_4 stretch	1728.4	1728.1	3
$\omega_4(a')$	C_2−C_3−C_4 bend	1277.2	1277.2	34
$\omega_5(a')$	C_3 rock	1116.3	1116.5	1
$\omega_6(a')$	H−C−C bend	947.2	947.1	4
$\omega_7(a'')$	H OPB	904.2	904.1	12
$\omega_8(a')$	C_4−C_5 stretch	680.8	680.8	3
$\omega_9(a'')$	C_5 OPB	532.9	532.8	1
$\omega_{10}(a')$	C_3−C_4−C_5 bend	530.1	530.1	1
$\omega_{11}(a'')$	N OPB	221.1	221.1	11
$\omega_{12}(a')$	N IPB	203.5	203.6	13
$\nu_1(a')$	C−H stretch	3136.5	3136.1	5
$\nu_2(a')$	C≡N stretch	2241.2	2241.0	1
$\nu_3(a')$	C_3−C_4 stretch	1685.6	1685.7	2
$\nu_4(a')$	C_2−C_3−C_4 bend	1244.4	1244.4	31
$\nu_5(a')$	C_3 rock	1087.3	1087.5	1
$\nu_6(a')$	H−C−C bend	924.3	922.2	5
$\nu_7(a'')$	H OPB	868.4	890.7	12
$\nu_8(a')$	C_4−C_5 stretch	671.9	671.4	4
$\nu_9(a'')$	C_5 OPB	533.3	528.8	1
$\nu_{10}(a')$	C_3−C_4−C_5 bend	522.7	523.8	1
$\nu_{11}(a'')$	N OPB	219.9	219.3	11
$\nu_{12}(a')$	N IPB	199.7	201.6	12

unaffected, and the rotational constants utilizing the cubic force constants are still negligibly affected.

The real problems typically arise in the anharmonic vibrational frequencies, which are the first observables to take advantage of the quartic force constants that suffer most from numerical issues. This is the case in the present work, to the extent that the OPB problem arises for these molecules. For c-C_3HF, the largest difference occurs in the H OPB in ν_6 at 4.0 cm^{-1} between the 0.005 and 0.010 rad step sizes. The next largest deviation is less than half that size at 1.7 cm^{-1} difference in the F IPB of ν_9. For c-C_3HCl, the only substantial difference between the 0.005 and 0.010 rad step sizes is again in the H OPB, with a difference of only 2.1 cm^{-1}. Across the two molecules, the largest change in moving from the 0.010 to 0.020 rad step size is 0.4 cm^{-1} in ν_6 of c-C_3HF. The rest of the changes between these larger step sizes are either 0.1 or 0.0 cm^{-1}, suggesting that the anharmonic frequencies are well-converged already at the 0.010 rad step size for coordinates S_8 and S_9 which contain the OPB motions. As such, only the 0.005 and 0.010 rad step sizes are utilized for the c-C_3HCN molecule.

Like c-C_3HF and c-C_3HCl, the deviations between step sizes for the harmonic frequencies of c-C_3HCN are negligible. The largest difference occurs in ω_1 where the 0.005 rad result is 0.4 cm^{-1} greater. The larger change in the harmonics relative to the previous molecules is portentous of the behavior of the anharmonic frequencies, but such a small deviation is still basically negligible in itself. In contrast to c-C_3HF and c-C_3HCl, though, the largest anharmonic difference in the H OPB (ν_7) is 22.3 cm^{-1} between the two step sizes. The C OPB similarly has a substantial change between the two of 4.5 cm^{-1}, but this is clearly much smaller, even relative to the magnitude of the frequency. The first of these accounts for a 2.5% difference between the step sizes, while the second is only 0.9%. The N OPB is basically unaffected with a change of only 0.6 cm^{-1} or 0.3% in relative terms. Between the previous work[56,57] and the trends observed for c-C_3HF and c-C_3HCl, it seems clear that the 0.010 rad step size should be more trustworthy. However, the affected H OPB has a relatively low intensity in all three molecules, so the accuracy of this fundamental is not particularly important for any observations regardless of their environments.

CONCLUSION

c-C_3HCN, c-C_3HF, and c-C_3HCl should be readily detectable in the ISM by both vibrational and rotational spectroscopies. All three molecules have dipole moments of roughly 3.0 D, enabling their rotational detection, although their dipole

https://doi.org/10.1021/acs.jpca.1c06576
J. Phys. Chem. A 2021, 125, 8860−8868

moments are slightly smaller than the 3.32 D of c-C_3H_2 itself. The available gas-phase experimental rotational constants for c-C_3HCN solidly corroborate the computed values for this molecule and support the accuracy of the F12-TZ QFF approach used herein for determining the same constants for c-C_3HF and c-C_3HCl for the first time. Unlike benzonitrile, which has a very intense C≡N stretch around 2242 cm^{-1}, c-C_3HCN has its most intense mode at 1244.4 cm^{-1} with an intensity of 34 km mol^{-1} but also exhibits a low intensity C≡N stretch at 2241.0 cm^{-1}. c-C_3HF and c-C_3HCl both have two C−C stretching modes with intensities of greater than 100 km mol^{-1} in the region between 1000 and 1800 cm^{-1}, well within the spectral range of the high-resolution EXES instrument on SOFIA. For c-C_3HF, these frequencies occur at 1765.2 and 1125.3 cm^{-1}, while the corresponding values for c-C_3HCl are at 1692.0 and 1062.5 cm^{-1}. These frequencies should serve as important identifiers for these molecules in potential future astronomical detections by NASA missions such as SOFIA and JWST. Such data are highly necessary given the previous detections of c-C_3H_2 and its ethynyl-functionalized form in the ISM.

■ ASSOCIATED CONTENT

Supporting Information

The Supporting Information is available free of charge at https://pubs.acs.org/doi/10.1021/acs.jpca.1c06576.

Fermi resonances and polyads, anharmonic constants, and force constants (PDF)

■ AUTHOR INFORMATION

Corresponding Author

Ryan C. Fortenberry − *Department of Chemistry & Biochemistry, University of Mississippi, University, Mississippi 38677-1848, United States;* orcid.org/0000-0003-4716-8225; Email: r410@olemiss.edu

Authors

Brent R. Westbrook − *Department of Chemistry & Biochemistry, University of Mississippi, University, Mississippi 38677-1848, United States;* orcid.org/0000-0002-6878-0192

Dev J. Patel − *Department of Chemistry & Biochemistry, University of Mississippi, University, Mississippi 38677-1848, United States*

Jax D. Dallas − *Department of Chemistry & Biochemistry, University of Mississippi, University, Mississippi 38677-1848, United States; Division of Chemistry and Chemical Engineering, California Institute of Technology, Pasadena, California 91125, United States*

G. Clark Swartzfager − *Department of Chemistry & Biochemistry, University of Mississippi, University, Mississippi 38677-1848, United States; Cleveland Central High School, Cleveland, Mississippi 38732, United States*

Timothy J. Lee − *MS 245-3, NASA Ames Research Center, Moffett Field, California 94035, United States;* orcid.org/0000-0002-2598-2237

Complete contact information is available at: https://pubs.acs.org/10.1021/acs.jpca.1c06576

Notes

The authors declare no competing financial interest.

■ ACKNOWLEDGMENTS

The present work is supported by NASA Grant NNX17AH15G and NSF Grant OIA-1757220. The Mississippi Center for Supercomputing Research (MCSR) graciously provided the computational resources. T.J.L. gratefully acknowledges the financial support from the 17-APRA17-0051, 18-APRA18-0013, and 18-2XRP18_2-0046 NASA grants. D.J.P. would also like to acknowledge support from the Ronald E. McNair Program at the University of Mississippi.

■ REFERENCES

(1) Thaddeus, P.; Gottlieb, C. A.; Hjalmarson, A.; Johansson, L. E. B.; Irvine, W. M.; Friberg, P.; Linke, R. A. Astronomical Detection of the C_3H Radical. *Astrophys. J.* **1985**, *294*, L49−L53.

(2) Madden, S. C.; Irvine, W. M.; Matthews, H. E.; Friberg, P.; Swade, D. A. A Survey of Cyclopropenylidene (C_3H_2) in Galactic Sources. *Astron. J.* **1989**, *97*, 1403−1422.

(3) Tielens, A. G. G. M. Interstellar Polycyclic Aromatic Hydrocarbon Molecules. *Annu. Rev. Astron. Astrophys.* **2008**, *46*, 289−337.

(4) Nixon, C. A.; Thelen, A. E.; Cordiner, M. A.; Kisiel, Z.; Charnley, S. B.; Molter, E. M.; Serigano, J.; Irwin, P. G. J.; Teanby, N. A.; Kuan, Y.-J. Detection of Cyclopropenylidene on Titan with ALMA. *Astronom. J.* **2020**, *160*, 205.

(5) Madden, S. C.; Irvine, W. M.; Matthews, H. E. Detection of ^{13}C-Substituted C_3H_2 in Astronomical Sources. *Astrophys. J.* **1986**, *311*, L27−L31.

(6) Gerin, M.; Wootten, H. A.; Combes, F.; Boulanger, F.; Peters, W. L., III; Kuiper, T. B. H.; Encrenaz, P. J.; Bogey, M. Deuterated C_3H_2 as a Clue to Deuterium Chemistry. *Astron. Astrophys.* **1987**, *173*, L1−L4.

(7) Spezzano, S.; Brünken, S.; Schilke, P.; Caselli, P.; Menten, K. M.; McCarthy, M. C.; Bizzocchi, L.; Trevinõ-Morales, S. P.; Aikawa, Y.; Schlemmer, S. Interstellar Detection of c-C_3H_2. *Astrophys. J., Lett.* **2013**, *769*, L19.

(8) Brown, R. D.; Godfrey, P. D.; Bettens, R. P. A. The Dipole Moment of C_3H_2. *Mon. Not. R. Astron. Soc.* **1987**, *227*, 19P−20P.

(9) Mebel, A. M.; Kislov, V. V.; Kaiser, R. I. Photoinduced Mechanism of Formation and Growth of Polycyclic Aromatic Hydrocarbons in Low-Temperature Environments via Successive Ethynyl Radical Additions. *J. Am. Chem. Soc.* **2008**, *130*, 13618−13629.

(10) Cernicharo, J.; Agúndez, M.; Cabezas, C.; Tercero, B.; Marcelino, N.; Pardo, J. R.; de Vicente, P. Pure Hydrocarbon Cycles in TMC-1: Discovery of Ethynyl Cyclopropenylidene, Cyclopentadiene, and Indene. *Astron. Astrophys.* **2021**, *649*, L15.

(11) McGuire, B. A.; Burkhardt, A. M.; Kalenskii, S.; Shingledecker, C. N.; Remijan, A. J.; Herbst, E.; McCarthy, M. C. Detection of the Aromatic Molecule Benzonitrile (c-C_6H_5CN) in the Interstellar Medium. *Science* **2018**, *359*, 202−205.

(12) Trevitt, A. J.; Goulay, F.; Meloni, G.; Osborn, D. L.; Taatjes, C. A.; Leone, S. R. Isomer-Specific Product Detection of CN Radical Reactions with Ethene and Propene by Tunable VUV Photoionization Mass Spectrometry. *Int. J. Mass Spectrom.* **2009**, *280*, 113−118.

(13) Rodríguez-Franco, A.; Martín-Pintado, J.; Fuente, A. CN Emission in Orion. The High Density Interface Between the H II Region and the Molecular Cloud. *Astron. Astrophys.* **1998**, *329*, 1097−1110.

(14) Snyder, L. E.; Buhl, D. Observations of Radio Emission from Interstellar Hydrogen Cyanide. *Astrophys. J.* **1971**, *163*, L47−L52.

(15) Agùndez, M.; Cernicharo, J.; Guèlin, M.; Kahane, C.; Roueff, E.; Klos, J.; Aoiz, F. J.; Lique, F.; Marcelino, N.; Goicoechea, J. R.; et al. Astronomical Identification of CN^-, the Smallest Observed Molecular Anion. *Astron. Astrophys.* **2010**, *517*, L2.

(16) McCarthy, M. C.; Grabow, J.-U.; Travers, M. J.; Chen, W.; Gottlieb, C. A.; Thaddeus, P. Laboratory Detection of the Ring-Chain Carbenes HC_4N and HC_6N. *Astrophys. J.* **1999**, *513*, 305−310.
(17) Tang, J.; Sumiyoshi, Y.; Endo, Y. Detection of the triplet HC_4N radical by Fourier Transform Microwave Spectroscopy. *Chem. Phys. Lett.* **1999**, *315*, 69−74.
(18) Aoki, K.; Ikuta, S.; Murakami, A. Most Stable Isomer and Singlet-Triplet Energy Separation in the HC_4N Molecule. *Chem. Phys. Lett.* **1993**, *209*, 211−215.
(19) Guèlin, M.; Thaddeus, P. Tentative Detection of the C_3N Radical. *Astrophys. J.* **1977**, *212*, L81−L85.
(20) Kaifu, N.; Ohishi, M.; Kawaguchi, K.; Saito, S.; Yamamoto, S.; Miyaji, T.; Miyazawa, K.; Ishikawa, S.; Noumaru, C.; Harasawa, S.; et al. A 8.8−50 GHz Complete Spectral Line Survey toward TMC-1 I. Survey Data. *Publ. Astron. Soc. Jpn.* **2004**, *56*, 69−173.
(21) Blake, G. A.; Keene, J.; Phillips, T. G. Chlorine in Dense Interstellar Clouds: The Abundances of HCl in OMC-1. *Astrophys. J.* **1985**, *295*, 501−506.
(22) Cernicharo, J.; Guélin, M. Metals in IRC +10216: Detection of NaCl, AlCl, and KCl, and Tentative Detection of AlF. *Astron. Astrophys.* **1987**, *183*, L10−L12.
(23) Federman, S. R.; Cardell, J. A.; Van Dishoeck, E. F.; Lambert, D. L.; Black, J. H. Vibrationally Excited H_2, HCl, and NO^+ in the Diffuse Clouds Toward ζ Ophiuchi. *Astrophys. J.* **1995**, *445*, 325−329.
(24) De Luca, M.; Gupta, H.; Neufeld, D.; Gerin, M.; Teyssier, D.; Drouin, B. J.; Pearson, J. C.; Lis, D. C.; Monje, R.; Phillips, T. G.; et al. Herschel/HIFI Discovery of HCl^+ in the Interstellar Medium. *Astrophys. J., Lett.* **2012**, *751*, L37.
(25) Fayolle, E. C.; Öberg, K. I.; Jørgensen, J. K.; Altwegg, K.; Calcutt, H.; Müller, H. S. P.; Rubin, M.; van der Wiel, M. H. D.; Bjerkeli, P.; Bourke, T. L.; et al. Protostellar and Cometary Detections of Organohalogens. *Nature Astron.* **2017**, *1*, 703−708.
(26) Savage, B. D.; Sembach, K. R. Interstellar Abundances from Absorption-Line Observations with the Hubble Space Telescope. *Annu. Rev. Astron. Astrophys.* **1996**, *34*, 279−329.
(27) Ziurys, L. M.; Apponi, A. J.; Phillips, T. G. Exotic Fluoride Molecules in IRC + 10216: Confirmation of AlF and Searches for MgF and CaF. *Astrophys. J.* **1994**, *433*, 729−732.
(28) Neufeld, D. A.; Zmuidzinas, J.; Schilke, P.; Phillips, T. G. Discovery of Interstellar Hydrogen Fluoride. *Astrophys. J.* **1997**, *488*, L141−L144.
(29) Neufeld, D. A.; Schilke, P.; Menten, K. M.; Wolfire, M. G.; Black, J. H.; Schuller, F.; Müller, H. S. P.; Thorwirth, S.; Güsten, R.; Philipp, S. Discovery of Interstellar CF^+. *Astron. Astrophys.* **2006**, *454*, L37−L40.
(30) Fortenberry, R. C.; Lee, T. J. Computational Vibrational Spectroscopy for the Detection of Molecules in Space. *Annu. Rep. Comput. Chem.* **2019**, *15*, 173−202.
(31) Raghavachari, K.; Trucks, G. W.; Pople, J. A.; Replogle, E. Highly Correlated Systems: Structure, Binding Energy and Harmonic Vibrational Frequencies of Ozone. *Chem. Phys. Lett.* **1989**, *158*, 207−212.
(32) Adler, T. B.; Knizia, G.; Werner, H.-J. A Simple and Efficient CCSD(T)-F12 Approximation. *J. Chem. Phys.* **2007**, *127*, 221106.
(33) Knizia, G.; Adler, T. B.; Werner, H.-J. Simplified CCSD(T)-F12 Methods: Theory and Benchmarks. *J. Chem. Phys.* **2009**, *130*, 054104.
(34) Huang, X.; Valeev, E. F.; Lee, T. J. Comparison of One-Particle Basis Set Extrapolation to Explicitly Correlated Methods for the Calculation of Accurate Quartic Force Fields, Vibrational Frequencies, and Spectroscopic Constants: Application to H_2O, N_2H^+, NO_2^+, and C_2H_2. *J. Chem. Phys.* **2010**, *133*, 244108.
(35) Agbaglo, D.; Lee, T. J.; Thackston, R.; Fortenberry, R. C. A Small Molecule with PAH Vibrational Properties and a Detectable Rotational Spectrum: c-(C)C_3H_2, Cyclopropenylidenyl Carbene. *Astrophys. J.* **2019**, *871*, 236.
(36) Agbaglo, D.; Fortenberry, R. C. The Performance of CCSD(T)-F12/aug-cc-pVTZ for the Computation of Anharmonic Fundamental Vibrational Frequencies. *Int. J. Quantum Chem.* **2019**, *119*, e25899.
(37) Agbaglo, D.; Fortenberry, R. C. The Performance of Explicitly Correlated Wavefunctions [CCSD(T)-F12b] in the Computation of Anharmonic Vibrational Frequencies. *Chem. Phys. Lett.* **2019**, *734*, 136720.
(38) Westbrook, B. R.; Fortenberry, R. C. Anharmonic Frequencies of $(MO)_2$ & Related Hydrides for M = Mg, Al, Si, P, S, Ca, & Ti and Heuristics for Predicting Anharmonic Corrections of Inorganic Oxides. *J. Phys. Chem. A* **2020**, *124*, 3191−3204.
(39) Gardner, M. B.; Westbrook, B. R.; Fortenberry, R. C.; Lee, T. J. Highly-Accurate Quartic Force Fields for the Prediction of Anharmonic Rotational Constants and Fundamental Vibrational Frequencies. *Spectrochim. Acta, Part A* **2021**, *248*, 119184.
(40) Werner, H.-J.; Knowles, P. J.; Manby, F. R.; Black, J. A.; Doll, K.; Heßelmann, A.; Kats, D.; Köhn, A.; Korona, T.; Kreplin, D. A.; et al. *MOLPRO, , a Package of Ab Initio Programs*, ver. 2020.1; 2020. http://www.molpro.net.
(41) Peterson, K. A.; Adler, T. B.; Werner, H.-J. Systematically Convergent Basis Sets for Explicitly Correlated Wavefunctions: The Atoms H, He, B-Ne, and Al-Ar. *J. Chem. Phys.* **2008**, *128*, 084102.
(42) Hill, J. G.; Peterson, K. A. Correlation Consistent Basis Sets for Explicitly Correlated Wavefunctions: Valence and Core-Valence Basis Sets for Li, Be, Na, and Mg. *Phys. Chem. Chem. Phys.* **2010**, *12*, 10460−10468.
(43) Møller, C.; Plesset, M. S. Note on an Approximation Treatment for Many-Electron Systems. *Phys. Rev.* **1934**, *46*, 618−622.
(44) Kendall, R. A.; Dunning, T. H.; Harrison, R. J. Electron Affinities of the First-Row Atoms Revisited. Systematic Basis Sets and Wave Functions. *J. Chem. Phys.* **1992**, *96*, 6796−6806.
(45) Frisch, M. J.; Trucks, G. W.; Schlegel, H. B.; Scuseria, G. E.; Robb, M. A.; Cheeseman, J. R.; Scalmani, G.; Barone, V.; Petersson, G. A.; Nakatsuji, H.; et al. *Gaussian 16*, rev. C.01; Gaussian Inc.: Wallingford, CT, 2016.
(46) Yu, Q.; Bowman, J. M.; Fortenberry, R. C.; Mancini, J. S.; Lee, T. J.; Crawford, T. D.; Klemperer, W.; Francisco, J. S. The Structure, Anharmonic Vibrational Frequencies, and Intensities of $NNHNN^+$. *J. Phys. Chem. A* **2015**, *119*, 11623−11631.
(47) Finney, B.; Fortenberry, R. C.; Francisco, J. S.; Peterson, K. A. A Spectroscopic Case for SPSi Detection: The Third-Row in a Single Molecule. *J. Chem. Phys.* **2016**, *145*, 124311.
(48) Allen, W. D.; et al. *INTDER*; 2005. INTDER is a general program written by W. D. Allen and co-workers which performs vibrational analysis and higher-order nonlinear transformations.
(49) Gaw, J. F.; Willets, A.; Green, W. H.; Handy, N. C. *SPECTRO Program*, ver. 3.0; 1996.
(50) Watson, J. K. G. In *Vibrational Spectra and Structure*; During, J. R., Ed.; Elsevier: Amsterdam, 1977; pp 1−89.
(51) Papousek, D.; Aliev, M. R. *Molecular Vibration-Rotation Spectra*; Elsevier: Amsterdam, 1982.
(52) Martin, J. M. L.; Taylor, P. R. Accurate *ab Initio* Quartic Force Field for trans-HNNH and Treatment of Resonance Polyads. *Spectrochim. Acta, Part A* **1997**, *53*, 1039−1050.
(53) Fortenberry, R. C.; Lee, T. J.; Layfield, J. P. Communication: The Failure of Correlation to Describe Carbon═Carbon Bonding in Out-of-Plane Bends. *J. Chem. Phys.* **2017**, *147*, 221101.
(54) Fortenberry, R. C.; Novak, C. M.; Layfield, J. P.; Matito, E.; Lee, T. J. Overcoming the Failure of Correlation for Out-of-Plane Motions in a Simple Aromatic: Rovibrational Quantum Chemical Analysis of c-C_3H_2. *J. Chem. Theory Comput.* **2018**, *14*, 2155−2164.
(55) Lee, T. J.; Fortenberry, R. C. The Unsolved Issue with Out-of-Plane Bending Frequencies for C═C Multiply Bonded Systems. *Spectrochim. Acta, Part A* **2021**, *248*, 119148.
(56) Westbrook, B. R.; Del Rio, W. A.; Lee, T. J.; Fortenberry, R. C. Overcoming the Out-of-plane Bending Issue in an Aromatic Hydrocarbon: The Anharmonic Vibrational Frequencies of c-(CH)C3H2+. *Phys. Chem. Chem. Phys.* **2020**, *22*, 12951−12958.
(57) Morgan, W. J.; Fortenberry, R. C.; Schaefer, H. F., III; Lee, T. J. Vibrational Analysis of the Ubiquitous Interstellar Molecule Cyclo-

https://doi.org/10.1021/acs.jpca.1c06576
J. Phys. Chem. A 2021, 125, 8860−8868

propenylidene (c-C_3H_2): The Importance of Numerical Stability. *Mol. Phys.* **2020**, *118*, 1.
(58) McCarthy, M. C.; Apponi, A. J.; Gordon, V. D.; Gottlieb, C. A.; Thaddeus, P.; Crawford, T. D.; Stanton, J. F. Rotational Spectrum and Theoretical Structure of the Carbene HC_4N. *J. Chem. Phys.* **1999**, *111*, 6750−6754.
(59) Becke, A. D. Density-Functional Thermochemistry. III. The Role of Exact Exchange. *J. Chem. Phys.* **1993**, *98*, 5648−5652.
(60) Yang, W. T.; Parr, R. G.; Lee, C. T. Various Functionals for the Kinetic Energy Density of an Atom or Molecule. *Phys. Rev. A: At., Mol., Opt. Phys.* **1986**, *34*, 4586−4590.
(61) Lee, C.; Yang, W. T.; Parr, R. G. Development of the Colle-Salvetti Correlation-Energy Formula into a Functional of the Electron Density. *Phys. Rev. B: Condens. Matter Mater. Phys.* **1988**, *37*, 785−789.
(62) Green, J. H. S.; Harrison, D. J. Vibrational Spectra of Benzene Derivatives-XVII. Benzonitrile and Substituted Benzonitriles. *Spectrochim. Acta* **1976**, *32A*, 1279−1286.

https://doi.org/10.1021/acs.jpca.1c06576
J. Phys. Chem. A 2021, 125, 8860−8868